

KASCADE extensive air shower experiment

H. Schieler^{b,*}, T. Antoni^a, W.D. Apel^b, F. Badea^{a,†}, K. Bekk^b, A. Bercuci^{b,†}, M. Bertaina^c,
H. Blümer^{b,a}, H. Bozdog^b, I.M. Brancus^d, C. Büttner^b, A. Chiavassa^c, K. Daumiller^a,
P. Doll^b, J. Engler^b, H. Falcke^g, M. Fessler^a, P.L. Ghia^e, H.J. Gils^b, R. Glasstetter^a,
R. Haeusler^a, A. Haungs^b, D. Heck^b, J.R. Hörandel^a, A. Horneffer^g, T. Huege^g, A. Iwan^{a,‡},
K.-H. Kampert^{a,b}, H.O. Klages^b, G. Maier^b, H.J. Mathes^b, H.J. Mayer^b, J. Milke^a,
C. Morello^e, M. Müller^b, G. Navarra^c, R. Obenland^b, J. Oehlschläger^b, M. Petcu^c,
H. Rebel^b, M. Roth^b, G. Schatz^b, J. Scholz^b, T. Thouw^b, G.C. Trinchero^e, H. Ulrich^a,
J.H. Weber^a, A. Weindl^b, J. Wentz^b, J. Wochele^b, J. Zabierowski^f, S. Zagromski^b

KASCADE-Grande and LOPES Collaborations

^aInstitut für Experimentelle Kernphysik, Universität Karlsruhe, 76021 Karlsruhe, Germany

^bInstitut für Kernphysik, Forschungszentrum Karlsruhe, 76021 Karlsruhe, Germany

^cDipartimento di Fisica Generale dell'Università, 10125 Torino, Italy

^dNational Institute of Physics and Nuclear Engineering, 7690 Bucharest, Romania

^eIstituto di Cosmo-Geofisica del CNR, 10133 Torino, Italy

^fSoltan Institute for Nuclear Studies, 90950 Lodz, Poland

^gMax-Planck-Institut für Radioastronomie, 53121 Bonn, Germany

ABSTRACT

The main aim of the KASCADE¹ extensive air shower (EAS) experiment is the determination of the chemical composition in the energy range around and above the *knee* of the primary cosmic ray spectrum. A large number of observables are measured simultaneously for each individual event, by the combination of various detection techniques for the electromagnetic, the muonic, and the hadronic component of the extensive air showers. Detailed investigations have been performed with the data measured by the KASCADE experiment since the start of data taking at the end of 1995. The results allow to evaluate hadronic interaction models, used in simulations to interpret air shower data. The all-particle spectrum of cosmic rays and their mass composition, as well as individual spectra for groups of elements have been reconstructed in the energy range between 10^{15} and 10^{17} eV. The results suggest, the *knee* in the all-particle cosmic-ray energy spectrum is caused by a rigidity-dependent cut-off of individual element groups. To improve the statistics around 10^{17} eV, where the "iron knee" in the cosmic ray spectrum is indicated in our data, the KASCADE experiment has recently been extended to KASCADE-Grande by a large collecting area (0.5 km^2) electromagnetic array, contributed from the former EAS-TOP² experiment. The Grande part will cover the primary energy range $10^{16} \text{ eV} < E_0 < 10^{18}$ eV, overlapping with KASCADE around 10^{16} eV, thus providing a continuous information from $3 \cdot 10^{14}$ eV to 10^{18} eV. In addition, new technologies in detecting radio emission from cosmic ray air showers will be tested by the LOPES collaboration at the site of KASCADE.

Keywords: KASCADE, EAS, air shower, cosmic ray, knee, LOPES, radio emission

1. INTRODUCTION

The earth's atmosphere is continuously bombarded by highly relativistic ionized particles, first discovered and named "cosmic rays" by V. Hess in 1912. Present-day experiments show the cosmic-ray energy spectrum

* Corresponding author; schieler@ik.fzk.de; phone +49 7247 82-3102; fax -3548; <http://www-ik.fzk.de/~schieler>

† on leave of absence from Nat. Inst. of Phys. and Nucl. Engineering, Bucharest, Romania

‡ on leave of absence from Department of Experimental Physics, University of Lodz, 90236 Lodz, Poland

extending up to more than 10^{20} eV. The flux spectrum follows a power law $dN/dE \propto E^{-\gamma}$ over many decades in energy. The most prominent feature is the *knee* in the spectrum around 3 PeV where the spectrum steepens from $\gamma \approx 2.7$ to $\gamma \approx 3.1$. The origin of cosmic rays is still under debate. Strong, relativistic shock fronts expanding from supernova explosions are favoured by popular models for the acceleration of ionized particles. Such models explain the particle acceleration up to energies of about $Z \cdot 10^{15}$ eV, with the nuclear charge Z of the particle. This upper limit coincides for primary protons with the mentioned steepening of the spectrum, and the origin of the *knee* is related to the upper limit of acceleration in several models.

Since the charged particles are deflected in the interstellar magnetic fields, the only hint of their sources are their energy spectrum and the mass composition, or more preferable, the energy spectra of individual elements. Cosmic rays at energies below 1 PeV have been directly observed by balloon-borne instruments at the top of the atmosphere or in outer space. At higher energies, the steep falling flux spectrum requires large detection areas or long observation periods, presently only possible in ground-based installations. These detector systems measure the secondary particles produced by cosmic rays in the atmosphere, the extensive air showers (EAS).

To investigate the cosmic rays from several 10^{13} eV up to 10^{17} eV the air shower experiment KASCADE has been built on-site at the Forschungszentrum Karlsruhe in Germany. The experiment detects the three main components of EAS simultaneously. A 200×200 m² field array³ measures the electromagnetic and muonic components. The 320 m² central detector system combines a large hadron calorimeter⁴ with several muon detection systems.⁵ In addition, high energetic muons are measured by an underground muon tracking detector.⁶

One of the main results so far obtained by the KASCADE (see Ref. 7–10) and EAS-TOP (see Ref. 11) experiments, is a picture of an increasingly heavier composition above the knee largely caused by a break in the spectrum of the light component. A change towards a heavier composition above the knee is expected in conventional acceleration models, where the knee is supposed to be rigidity dependent. A convincing verification of this type of model would be the observation of the knee in the heavy component in the primary energy region around $E_0 = Z_{Fe} \times E_k \approx 10^{17}$ eV. Such an uncovering requires the extension of the high quality data obtained in the energy range 10^{15} - 10^{16} eV by KASCADE and EAS-TOP, without losing accuracy, significantly above E_0 . For this purpose, a new array (called Grande) is being realized by means of 37 stations of 10 m² each of scintillator counters at a mutual distance of about 130 m and covering globally an area of about 0.5 km², next to the KASCADE site in order to operate jointly with the existing KASCADE detectors. In this configuration the Grande part will cover the primary energy range $10^{16} \text{ eV} < E_0 < 10^{18} \text{ eV}$.

The main task is the observation of the "iron knee", which is expected following the increasing mass of the primaries observed between 10^{15} and 10^{16} eV (*knee* region for the light component), and the rigidity dependent breaks for the spectra of different primaries from the conventional acceleration models. Its observation will provide a definite proof of the *knee* structure. The superposition with KASCADE will guarantee the cross calibration of the detectors, and provide a full coverage from $3 \cdot 10^{14}$ to 10^{18} eV for the KASCADE-Grande experiment. It will start operation in January 2003, and will reach its full statistics in 3-4 years of data taking.

To test and demonstrate the capability of new technologies in detecting radio emission from cosmic ray air showers, a prototype station with 10 antennas will be built up by the LOPES collaboration at the site of KASCADE in the next months and operated in conjunction with it. It is planned to extend it in a second phase until 2004 to 100 antennas.

2. THE KASCADE EXPERIMENT

KASCADE (Karlsruhe Shower Core and Array Detector) is located on the laboratory site of the Forschungszentrum Karlsruhe, Germany (at 8° E, 49° N, 110 m a.s.l.). The experiment consists of several, nearly independent parts. Its schematic layout is shown in Fig. 1 (left) with the three main components: field array, central detector system, and muon tracking detector.

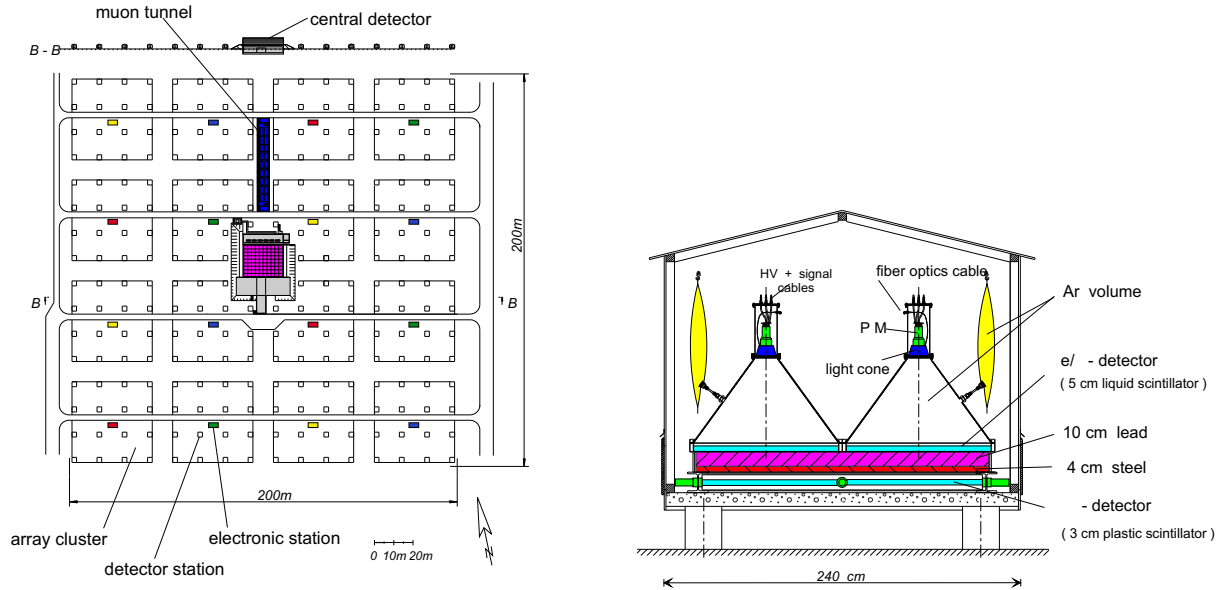


Figure 1. Schematic layout of the KASCADE experiment (left). KASCADE field array detector station (right).

2.1. The Field Array

Scintillation detectors for the measurement of the electrons and photons and of the muons outside the core region of the extensive air showers are housed in 252 detector stations on a rectangular grid with 13 m spacing forming a field array of $200 \times 200 \text{ m}^2$. A station (Fig. 1 (left)) contains four scintillation detectors for the electron/photon component (Fig. 2) with a total area of about 3.2 m^2 on top of a thick absorber plate. About 38 l of custom made liquid scintillator in each stainless steel container of 100 cm diameter give a thickness of 48 mm. These detectors have been optimized for good resolution in energy - about 8% at 12 MeV, the mean energy deposit of a minimum ionising particle (m.i.p.) - and in time (0.8 nsec) as well as for a very high dynamic range. Energy deposits equivalent to 2000 m.i.p. can be detected linearly with a threshold of 0.25 m.i.p. (3 MeV). The absorber of 10 cm of lead and 4 cm of iron corresponds to more than 20 radiation lengths and to a muon threshold of about 0.3 GeV. The 3.2 m^2 muon detector below the shielding consists of 4 sheets of plastic scintillator, $90 \times 90 \times 3 \text{ cm}^3$ each, read out by green wavelength shifter bars on all edges with a total of 4 phototubes (Fig. 2).

The supply and the electronic readout of the detectors in the stations is organized in 16 clusters of 16 stations - 15 stations in the inner 4 clusters of the experiment (see Fig. 1 (left)). These clusters act as independent air shower field arrays. The detector control and readout is performed locally using transputer based VME controllers (TVCs). The fast transputer links are connected in the central data acquisition system to a workstation host.

In the present setup of KASCADE only the 60 stations in the 4 clusters near the central detector are equipped with four electron detectors, whereas the outer 12 clusters contain two detectors/station only. Trigger conditions¹² are a cluster detector multiplicity \mathbf{n} of 32 (\mathbf{m} of 60 in the inner 4 clusters) or a local high energy deposit in one station. In the inner 4 clusters the absorber plates and the muon detectors are not installed. The detector areas at present are 490 m^2 for the electromagnetic and 622 m^2 for the muon component of the extensive air showers. The measurement of the energy deposit in the scintillators and of the arrival time of the first shower particle in a station was supplemented by the installation of 16 Flash ADCs (1 Gs/s)¹³ in one cluster for the determination of the time distributions of the electrons and muons in the showers.

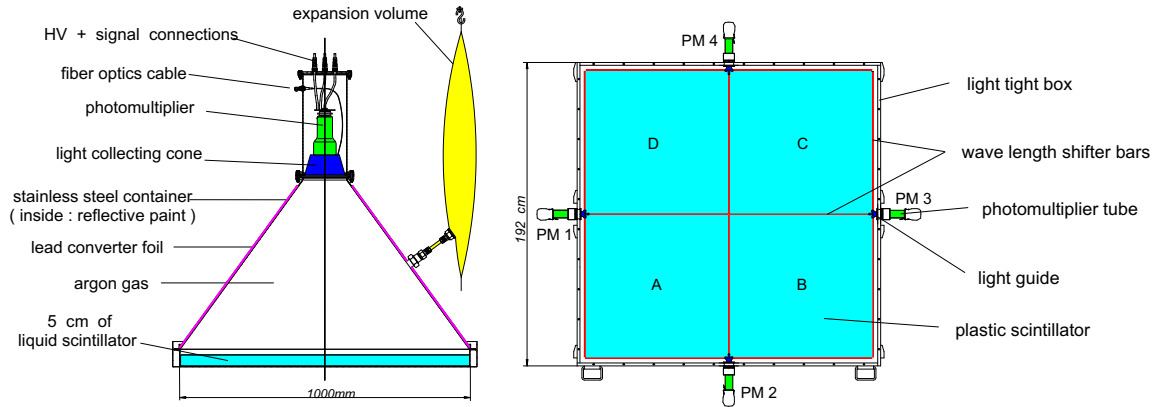


Figure 2. The liquid scintillation detectors for the electromagnetic shower component (left) and the muon detectors (right) of the field array.

2.2. The Central Detector System

The main part of the central detector system (Fig. 3) is the fine segmented hadron calorimeter. It consists of a $20 \times 16 \text{ m}^2$ iron stack (4,000 tons) with 8 horizontal gaps.

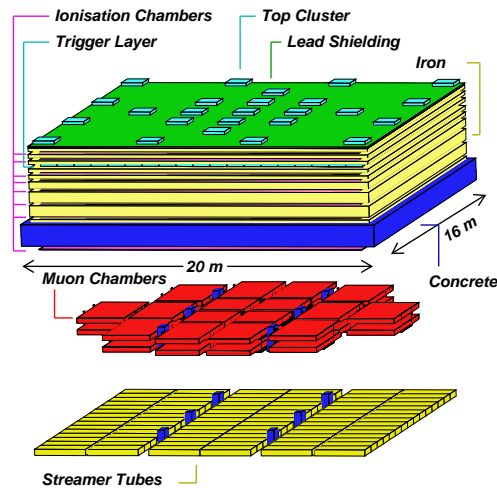


Figure 3. Schematic layout of the central detector system of KASCADE.

10,808 ionization chambers filled with the room temperature liquid tetramethylsilane (TMS) or tetramethylpentane (TMP) are used for the measurement of hadronic energy in the gaps^{4, 14} and in the additional layer on top. A schematic view of a TMS/TMP chamber is shown in Fig. 4 (left). Each chamber has the size $50 \times 50 \times 1 \text{ cm}^3$ and contains 4 electrodes of $25 \times 25 \text{ cm}^2$. Thus the readout of the calorimeter amounts to 43.232 electronic channels. The fine segmentation enables the separation of hadrons with a distance as low as 50 cm. The amplifier chain has a dynamic range of 10^4 and its feed back performance ensures a very stable operation over many years. The thickness of the iron stack of about 1.7 m corresponds to more than ten nuclear interaction lengths. The top layer of ionization chambers is unshielded and the 2nd layer is shielded by 12 cm of iron and additional 5 cm of lead against the electromagnetic component of the showers.

The calorimeter is able to measure the energy of vertical hadrons with about 10% accuracy in the range from 100 GeV to more than 10 TeV. An example of a transition curve for a single hadron of 1 TeV is shown

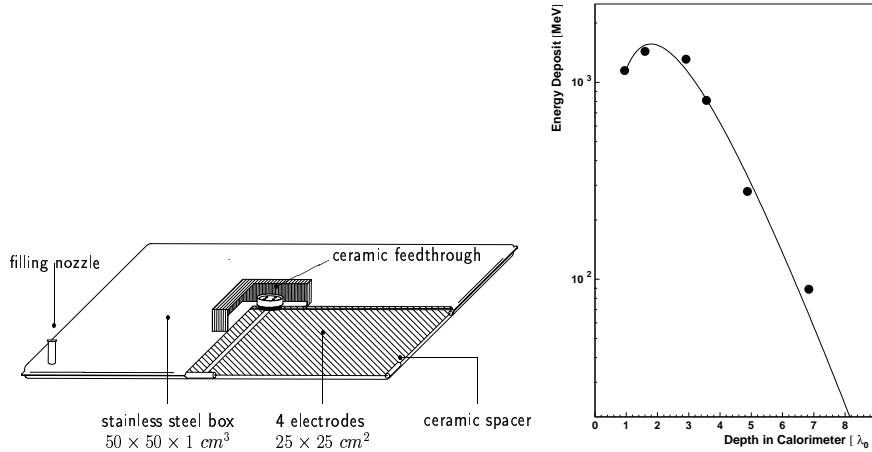


Figure 4. Schematic view of a TMS/TMP chamber of the central hadron calorimeter (left). The transition curve of a 1 TeV hadron in the iron - TMS/TMP calorimeter (right).

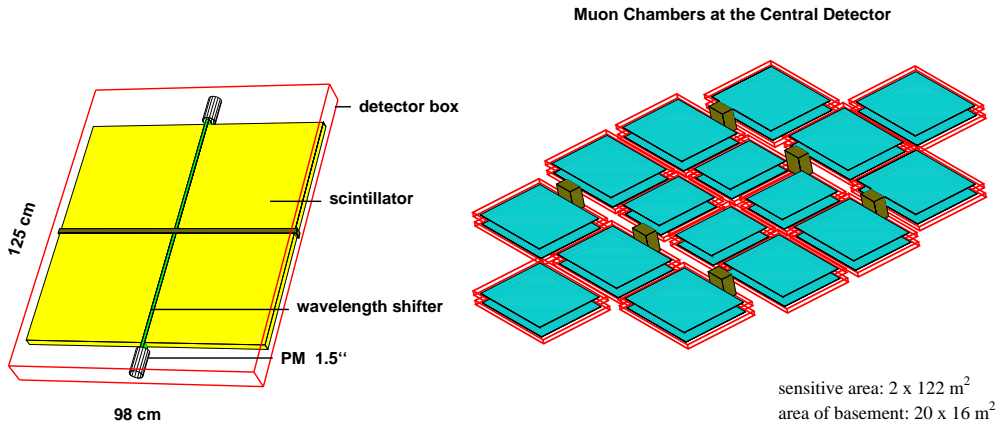


Figure 5. The scintillation detectors of the central detector trigger layer and the top cluster (left). Two layers of Muon Chambers (MWPCs) measure muon tracks in the basement of the central detector (right).

in Fig. 4 (right). The angle of incidence can be reconstructed to 1.5° . The energy sum of the hadrons in the core of a 1 PeV shower can be determined with a resolution of 8%. Individual hadrons with energies down to 20 GeV are reconstructed. In this energy range 70% of all hadrons are found.

In the third gap from the top of the iron stack (shielded by about 30 r.l.) a layer of 456 scintillation detectors is placed. Each detector contains two sheets of plastic scintillator read out by a green wavelength shifter bar and a single photomultiplier (Fig. 5 (left)). The module area is 0.45 m^2 , the time resolution 1.8 nsec. The scintillator layer is used for the triggering of the calorimeter readout in two different ways. A hadron trigger is accepted, if in one of the modules the energy deposit is more than 300 MeV (50 m.i.p.). By this trigger, also single hadrons can be detected. The second possibility is a muon multiplicity trigger when n of the 456 detector modules have a signal larger than 1 m.i.p..

The trigger layer acts, in addition, as a 200 m^2 compact hadron and muon detector with rather high segmentation and good time resolution. In large showers with cores far outside the central detector, the lateral and time distributions of the muons will be determined¹⁵ with a threshold of about 0.5 GeV and of 2.4 GeV, when combined with the MWPC information (see below). Especially for lower energy events, the arrival times of the individual hadrons and muons in the shower core can be measured.

Below the iron stack and the base of the calorimeter, two layers of multiwire proportional chambers (MW-

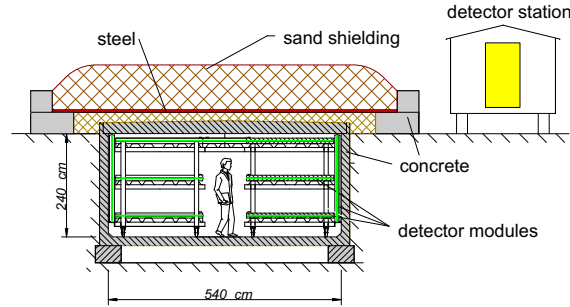


Figure 6. Muon tracks are measured by the muon tracking detector (MTD) with three layers of streamer tubes in a shielded tunnel.

PCs), called the Muon Chambers⁵, are used for the measurement of muon tracks with an accuracy of about 1.0° and a muon threshold of 2.4 GeV. The MWPCs cover a total area of 122 m^2 as shown in Fig. 5 (right). Since they are position sensitive they allow to measure the lateral distribution of the observed particles with a spatial resolution of a few mm. The determination of position is done by crossed anode wires and cathode stripes. The studies using the MWPCs have been limited by their size, as they cover only about 40% of the area of the central detector system, and also by the ability to resolve multiple particle hits. Ambiguities occur above a particle density of 2 m^{-2} . As a result of these ambiguities only particle densities in a range of up to 4 m^{-2} can be measured. To improve this situation an additional layer of limited streamer tubes (LST)¹⁶ has been installed below the muon chambers, increasing the detector area and the resolution of ambiguities of the hit reconstruction. The LSTs cover a total area of 300 m^2 . The MWPC and LST readout can be triggered either from the trigger layer or from the trigger signal of one of the field array clusters. A third possibility is a trigger from the top cluster, a group of scintillation detectors above the central detector.

50 scintillation detectors of the same type as in the trigger layer form the top cluster above the calorimeter. This system is used for the measurement of small central showers with sizes below the threshold of the field array. It will also supply the information on the charged particle densities in the area of the central detector, where 4 stations of the field array are missing.

2.3. The Muon Tracking Detector

North of the central detector a 50 m long and 5.5 m wide tunnel has been added to the experiment. In this tunnel 600 m^2 of limited streamer tubes are used in three layers for the tracking of muons under a shielding of concrete, iron, and sand (Fig. 6), corresponding to 18 r.l. and a muon threshold of 0.8 GeV. The tracking accuracy is around 0.5° . The detector⁶ has an effective area of about 150 m^2 for the determination of the size and lateral distribution of the muon component in EAS and will, in addition, enable by triangulation the approximate determination of the mean muon production height, especially for showers with energies above 10^{16} eV . Shower simulations with the CORSIKA¹⁷ code show, that this observable is strongly dependent on the mass of the primary particle. Due to the multiple scattering of the muons in the air and in the shielding above the detectors, at least 30 muons have to be detected at a typical distance of 100 - 150 m from the shower core for a sufficiently precise determination of the mean angle of incidence. Therefore, this method is restricted mainly to large showers.

2.4. Data Handling and Correlation

The 16 clusters of the field array, the muon tracking detector and the five parts of the central detector system are (in principal) 22 independent experiments, which can be started, run, read out and stopped alone or together.¹⁸ To correlate the data from different parts of KASCADE, common clock signals are used. They are derived from a GPS receiver and a Rubidium high frequency generator. Synchronized pulse trails of 1 Hz and of 5 MHz are distributed via fiber optic cables to all parts of the KASCADE experiment. 5 MHz counters are used in every frontend electronics system. For each detector event the contents of these counters are read and added to the

data as time labels. The UTC time of each shower is also recorded - the 1 Hz pulses are used to increment a time scaler which is preset appropriately when the experiment parts are started.

In case of a trigger the event data (including the time labels) are transferred from the local processors to a central workstation, where they are checked for time labels in a preset interval around the trigger time. Eventbuilder software is used on the host to correlate the data before transferring them to a mass storage device. A large number of other online tasks like detector control and calibration, track reconstruction etc. can also be performed on the processor net. The event display is handled on the central workstation.

2.5. Trigger Sources - Rates - Thresholds

The different trigger sources in the KASCADE experiment can be used to study a broad variety of physics problems. The single hadron trigger of the central detector trigger layer with a rate of about 0.5 sec^{-1} is used to study the flux spectrum of unaccompanied high energy hadrons. The top cluster and the field array detectors are used to select clean single hadron events. The simulations show that these events allow to study the energy range of 1 TeV and higher for the primary particles.

The top cluster multiplicity trigger (\mathbf{n} of 50) is used to read out the whole experiment in the case of low energy central shower events. This enables the detailed and complete study of all components of showers with energies typically larger than 10^{13} eV. In this energy range the predictions from extensive air shower simulation codes like CORSIKA can be tested most efficiently. The number and distribution of muons and hadrons in the cores of these showers can be determined with good accuracy.

The main trigger source for the study of the primary spectrum and the composition around the knee is a detector multiplicity (\mathbf{n} of 32 ; \mathbf{m} of 60) fulfilled in at least one cluster of the field array.

A typical trigger requirement used at present is $\mathbf{n} = 10$ to 15, $\mathbf{m} = 20$ to 30, corresponding to rates of 1 to 3 sec^{-1} . The resulting threshold of the measurements is a few times 10^{14} eV, depending on zenith angle and primary mass. The upper limit of the energy range of the KASCADE experiment is defined by the size of the field array. We expect about one event/day at 10^{17} eV. In most cases the field array trigger will be accompanied by a muon multiplicity trigger from the trigger layer in the central detector.

The muon tracking detector in the tunnel can produce its own muon multiplicity trigger, but normally the readout is triggered from the field array clusters or the central detector system.

In the field array, a local high energy deposit in one station can be used as a trigger condition also. This can be used to study very narrow events.

2.6. Experimental Observables

The main strength of KASCADE lies in the large number of experimental quantities which can be measured simultaneously for each event. This enables multidimensional analyses for the determination of the basic properties of the event, the energy and the mass of the primary.

The most straightforward measurements are the determination of the **absolute time** of the event, of the **position of the shower core** and of the **zenith and azimuth angle**. The **electron size** of the shower and the lateral distribution of the electrons (the **shower age**) can be determined. The **density of muons** can be measured both in the shower core and in the outer parts. In the shower cores, the **number and lateral distribution of hadrons** as well as the **hadron energy** are important quantities. **Arrival time distributions of hadrons, muons, and electrons** can be measured. In the shower cores the **pattern of the muon hits** can be studied. For higher energy events a determination of the muon **lateral distribution** parameter and of the **muon angle** relative to the shower axis will be possible. In the field array the details of the distribution of electrons like (delayed) **subshowers**, asymmetric events, multiple cores or narrow events can be studied. The use of different muon detection techniques with thresholds from 0.23 to 2.4 GeV gives at least some information on the **muon energy** distribution in the EAS.

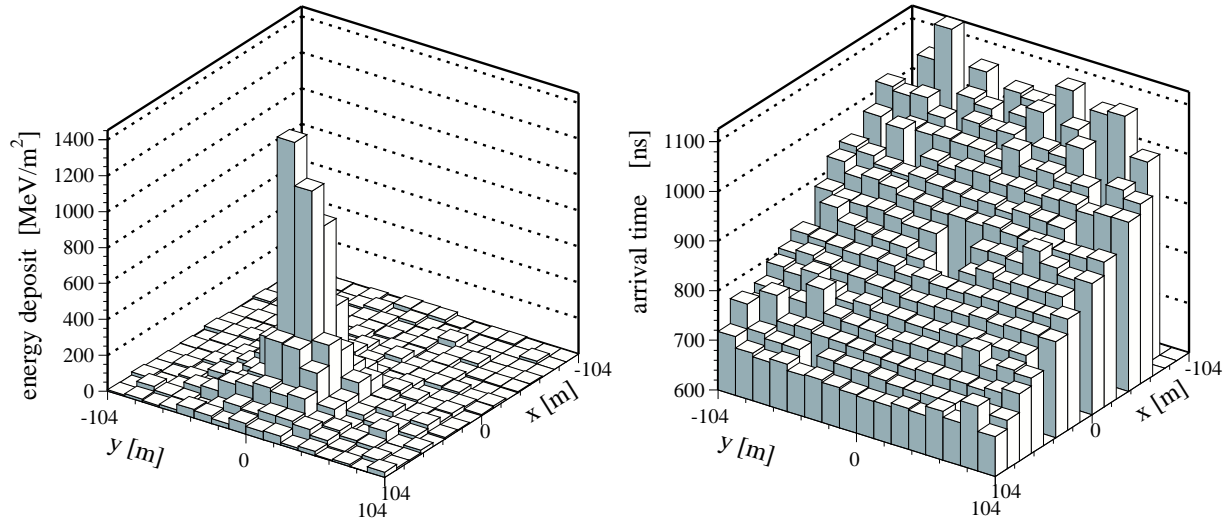


Figure 7. Energy deposits (left) and arrival times (right) of the particles in an EAS measured by the electron detectors of the field array. The reconstructed values are: number of electrons $N_e = 258000$; shower age parameter $s = 1.05$; shower core at $x_c = 40$ m, $y_c = 0.6$ m; shower direction $\Theta = 32.6^\circ$, $\Phi = 102^\circ$; (Run 496, Event 55534).

2.7. Event Reconstruction

The off-line analysis of the shower events is performed using a program based on standard routines and data structures used in many high energy physics experiments. The code KRETA has been developed to analyse the raw data from all parts of KASCADE in several steps (levels). In the first, fast level the data calibration and correction procedures are performed. Muon and hadron tracks are identified and reconstructed and energies assigned to the hadron tracks. The core position and the shower direction are determined from the calibrated field array data (see Fig. 7) using fast algorithms like a neural network and a gradient method^{19,20}. Electron and muon numbers are estimated using fast empirical approaches.

In the second level fits are performed to the data, e.g. various analytic functions to the lateral distributions of electrons and muons, a cone fit to the shower front, etc.. In this step the main shower parameters like particle densities, distributions, are determined. The event reconstruction is continued in a correlated multiparameter analysis of the measured observables using a broad variety of methods. Cuts are performed to the data, the principal components of the parameter space are determined, neural network reconstruction methods will be applied, nonparametric (Bayes) classification schemes are used, and fractal moments of the muon and hadron distributions are determined²¹. This part of the analysis procedure is improved further as our experimental understanding of the details of extensive air shower events is growing.

2.8. Reconstruction Accuracy

To estimate the accuracy of the reconstructed shower parameters, some effort has been put into the understanding of the detector response to extensive air showers. The event simulation code CRES has been developed, based on the GEANT3 package. As input to CRES simulated air shower data from CORSIKA are used. Due to the fast improvement of computing power in the recent years detailed simulations of EAS for different primaries, zenith angles and primary energies and of the detailed response of the KASCADE experiment to these events could be performed with sufficient statistical accuracy. With these calculations it was possible to test and improve the different reconstruction methods and to study the origin of many systematic effects. It turned out that in general the reconstruction gets better for larger showers - sampling fluctuations get less important.

The numbers quoted below are relative errors for showers with electron size greater than 10^5 , which corresponds to about 10^{15} eV in our case. For these events the hadronic energy sum in the shower core is determined to an accuracy of 5%, the number of hadrons to 8% and the muon number (above 2.4 GeV) in the core to 12%,

if the shower core falls inside the central detector. The shower disk is measured by the field array with an error of 8% for the electron size, of 7% for the age parameter, and of 16% for the muon number. The core position is determined with an accuracy of about 2.5 m and the direction of the shower to better than 0.3° .

2.9. Measurements and Results

Data taking has started at the end of 1995. Until now, more than 500 million events (air showers) have been measured and stored on mass storage systems. From the experimental data several observables have been reconstructed. We will focus in this paper on only two aspects out of a large number of investigations.

2.9.1. Investigation of hadronic interactions

In order to obtain the mass and energy of the shower-inducing particle, measured EAS observables are compared with predictions of simulations. These simulations describe the development of an EAS in the atmosphere and, thereafter, the signal response for all individual particles hitting the detectors. A critical part in the simulation chain is the model used to describe the high-energy hadronic interactions, since the model has to extrapolate into kinematical and energy regions not covered by present-day collider experiments. The Karlsruhe EAS simulation program CORSIKA¹⁷ provides several high-energy hadronic interaction models — HDPM, DPMJET, NEXUS, QGSJET, SIBYLL, VENUS — based on different phenomenological descriptions. Below 80 GeV the codes GHEISHA and URQMD are available. One objective of the KASCADE experiment is to evaluate these models and to provide criteria for their improvement.

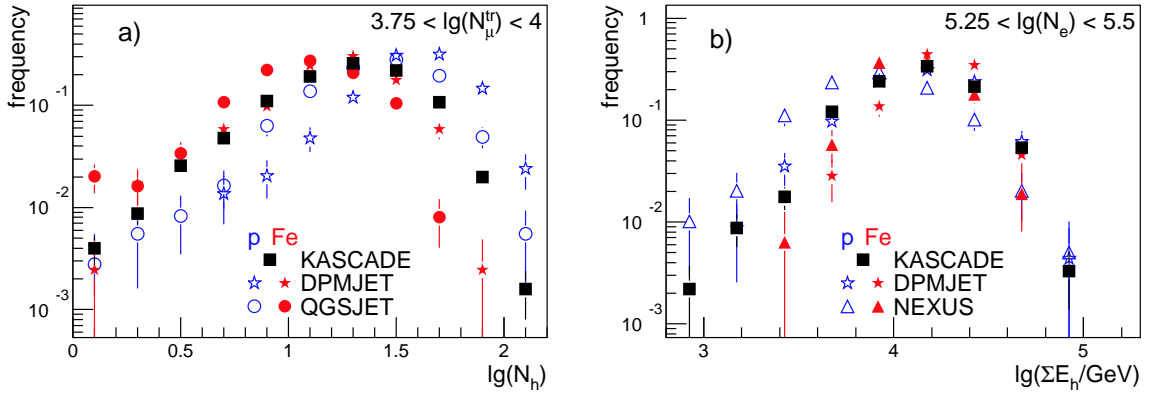


Figure 8. Frequency distribution for a) the number of reconstructed hadrons and b) their energy sum in EAS for two shower size intervals²².

The hadron calorimeter is a valuable detector for testing the interaction models. The structure of the hadronic component is examined in energy and spatial coordinates. Observables used include the number of hadrons as well as their energy sum, their lateral distribution and their energy spectrum, the energy of each individual hadron relative to the most energetic hadron in an EAS, the maximum hadron energy, and the spatial distribution of the hadrons. All observables are investigated as functions of the number of electrons and muons as well as of the hadronic energy sum.

An example of such investigations is given in Fig. 8. Shown are frequency distributions for the number of reconstructed hadrons above 50 GeV and the hadronic energy sum for two shower size intervals for EAS with shower core inside the calorimeter. KASCADE findings are compared with predictions of the models QGSJET, DPMJET, and NEXUS for two extreme mass scenarios, the primaries being only protons or iron nuclei²². Combining all observables, it turned out that the model QGSJET delivers the most reliable description^{22, 23}. This model is used for the analyses described in the following sections.

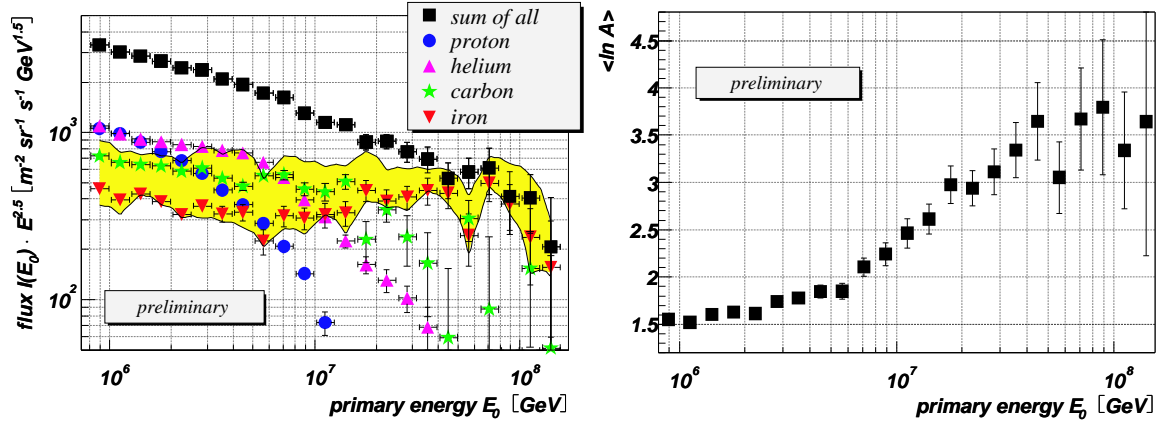


Figure 9. Cosmic ray energy spectrum for four groups of elements and the resulting all-particle spectrum²⁷ (left) and mean logarithmic mass vs. energy (right) calculated from individual spectra for four groups of elements as shown in the left figure²⁷.

2.9.2. Energy spectra and mass composition

Several analysis methods have been carried out to obtain the cosmic-ray energy spectrum. The KASCADE data show a *knee* in the electromagnetic, muonic, and hadronic shower size spectra²⁴. From the size spectra, the primary energy spectrum has been derived (see e.g. Ref. 25), including the absolute flux spectrum obtained for the first time using hadronic observables²⁶.

A recent analysis²⁷ uses electromagnetic and muonic shower size spectra in three different zenith angle bins. With a four component assumption for the mass composition of primary cosmic rays (protons, helium, CNO-group, and iron group), an unfolding algorithm is applied, taking into account shower fluctuations and experimental effects. The hadronic interactions have been simulated using the model QGSJET above 80 GeV and the GHEISHA code below. Individual energy spectra for the four mass groups are obtained as shown in Fig. 9 (left). Each spectrum shows a *knee*-like structure. The energy dependence of these cut-offs suggests a rigidity-dependent behaviour. The mean logarithmic mass calculated from the individual energy spectra is shown in Fig. 9 (right), indicating an increase of the average mass above the *knee*.

3. KASCADE-GRANDE: EXTENDING THE EXPERIMENT

The basic layout of KASCADE-Grande is reported in Fig. 10 (left). It consists of three different arrays: KASCADE, Grande, and Piccolo.

Grande consists of 37 stations of 10 m² each of scintillator counters - basically the electromagnetic detector of EAS-TOP² - at a mutual distance of about 130 m and covering globally an area of about 0.5 km² next to the KASCADE site. Each of the 10 m² station is split into 16 individual scintillators (NE102A, 80 × 80 cm² area, 4 cm thick). Each scintillator is viewed by a photomultiplier XP3462B for timing and particle density measurements from $n_p \approx 0.3$ to ≈ 750 /10 m⁻² (HG ch). The four central scintillators are equipped with an additional similar PM but with a maximum linearity divider, for large particle density measurements: from $n_p \approx 12$ to ≈ 30000 /10 m⁻² (LG ch).

Piccolo consists of an array of 8 huts (10 m² each) equipped with 12 scintillator plates each, placed towards the center of the Grande array. Each hut is logically and electronically divided into 2 stations. From the view of the data acquisition it is equipped and acts like a 2nd field array with only one cluster, whereas the detectors are different. The main aim of Piccolo is to provide an external trigger to Grande and KASCADE for coincidence events allowing the recording of data from all the detectors of KASCADE-Grande. A triggering condition of ≈ 1 Hz will provide an efficiency $\epsilon > 0.6$ at 10¹⁶ eV, becoming $\epsilon \approx 1$ at $5 \cdot 10^{16}$ eV for all primaries in the fiducial area of 300 m radius around Piccolo (from CORSIKA-QGSJET).

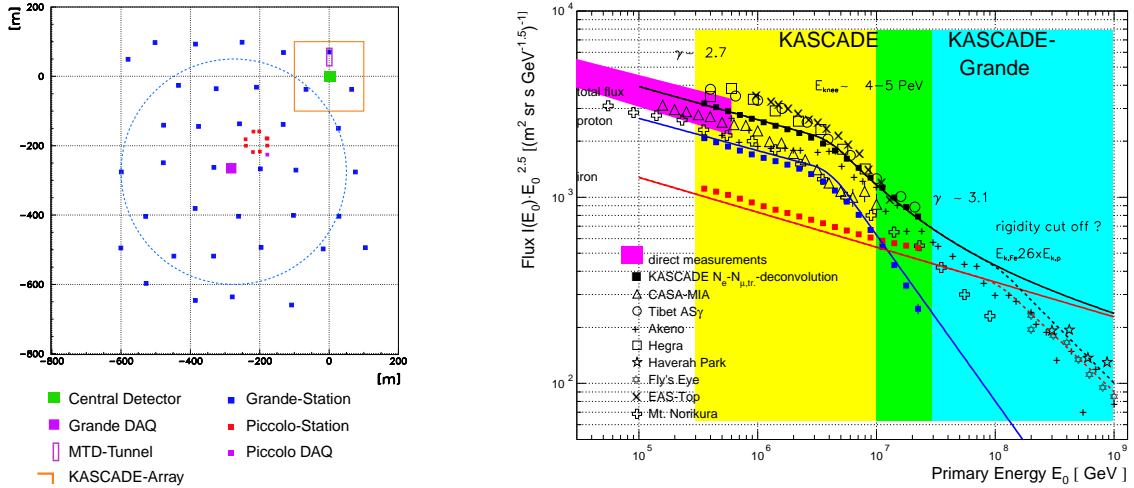


Figure 10. Layout of KASCADE-Grande (left). Differential energy spectrum of CRs. The knee of the light component, the expectation for the heavy one, and the energy region covered by the KASCADE and KASCADE-Grande arrays are shown. The darker area represents the region of superposition of the two detectors (right).

Piccolo, Grande and the cross triggering electronics are under construction, and the full array will start common data taking in January 2003.

The energy range of interest is shown in Fig.10 (right). With three years data taking, and collecting area $A \simeq 0.5 \text{ km}^2$, the total exposure of KASCADE-Grande will be: $\Gamma \simeq 10^{14} \text{ m}^2 \text{ srs}$. This will correspond to a collected number of events (including the trigger efficiency of Piccolo): $n(> 10^{16} \text{ eV}) \simeq 1.7 \cdot 10^6$, $n(> 3 \cdot 10^{16} \text{ eV}) \simeq 2.8 \cdot 10^5$, $n(> 10^{17} \text{ eV}) \simeq 2.5 \cdot 10^4$, $n(> 3 \cdot 10^{17} \text{ eV}) \simeq 2.8 \cdot 10^3$, $n(> 10^{18} \text{ eV}) \simeq 250$. Up to about 10^{18} eV KASCADE-Grande will thus provide statistically significant physical information.

The basic observables will be: the muon density at core distance between 300 and 600 m (providing, together with the observed muon lateral distribution, the muon density at 600 m, $D_{\mu 600}$), their reconstructed production heights (h_{μ}) from the tracking modules (including timing information for the muons in the KASCADE central detector), and the shower size (N_e) and lateral electron density profile from the extended electromagnetic (e.m.) array.

4. DETECTING RADIO EMISSION FROM COSMIC RAY AIR SHOWERS

4.1. Radio Properties of EAS

Radio emission from cosmic ray air showers were discovered for the first time by Jelly et al.²⁸(1965) at 44 MHz. The results were soon verified and in the late 1960's emission from 2 MHz up to 520 MHz were found. In the following years these activities ceased almost completely due to several reasons: difficulty with radio interference, uncertainty about the interpretation of the results and the success of other methods.

The radio properties of extensive air showers are summarized in an excellent review by Allan²⁹(1971). The main results of this review can be summarized by an approximate formula relating the received voltage to various other parameters:

$$\epsilon_{\nu} = s \left(\frac{E_p}{10^{17} \text{ eV}} \right) \exp \left(\frac{-R}{R_0(\nu, \theta)} \right) \cos \theta \sin \alpha \left(\frac{\nu}{55 \text{ MHz}} \right)^{-1} \left[\frac{\mu V}{\text{m MHz}} \right] \quad (1)$$

Here E_p is the primary particle energy, R is the distance to the shower center, R_0 is around 110 m at 55 MHz, θ is the zenith angle, α is the angle of the shower axis to the geomagnetic field and ν is the observing frequency. The value of the calibration factor s is still not know, due to uncertainties in the primary energy calibration.

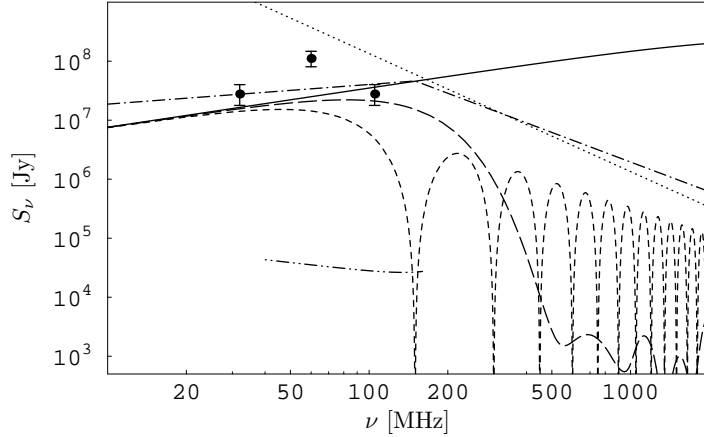


Figure 11. Equivalent flux density spectrum of a 10^{17} eV shower. Dotted: ν^{-2} formula from Allan²⁹(1971); Dash-dotted: Falcke&Gorham³⁰(2002) approximation; Solid: geosynchrotron emission with full coherence; Short-dashed: same with uniform 2 m line-charge; Long-dashed: same with Gaussian 2 m line-charge; Dash-2x-dotted: LOPES 100 station RMS noise; Data points from Prah³¹(1971).

Values of $1.6 < s < 20$ are reported. This formula was determined experimentally from data in the energy range $10^{16} < E_p < 10^{18}$ eV at a frequency of ≈ 55 MHz.

The spectral form of the radio emission is still not clear, also the emission process is still not known. Although the dependence on the geomagnetic field suggests coherent synchrotron radiation in the Earth's magnetic field (see Ref. 30), other processes like Cherenkov radiation are also possible.

In Fig. 11[§] the radio power spectrum from the Allan-formula ($\epsilon_\nu \sim \nu^{-1} \Rightarrow S_\nu \sim \nu^{-2}$), the approximation from Falcke&Gorham³⁰(2002), results from geosynchrotron emission modeling for different air shower geometries (see Ref. 32) and some data points for low frequencies are shown.

4.2. LOFAR and LOPES

The **Low Frequency Array** (LOFAR)³³ is a new attempt to revitalize astrophysical research at 10-200 MHz. The basic idea of LOFAR is to build a large array of 100 stations of 100 dipoles in which the received waves are digitized and sent to a central super-cluster of computers.

A new feature is the possibility to store the entire data stream for a certain period of time. If one detects a transient phenomena like an air shower one can then retrospectively form a beam in the desired direction and thus basically look back in time. LOFAR therefore combines the advantages of a low-gain antenna (large field of view) and a high-gain antenna (high sensitivity and background suppression).

To test this technology and demonstrate its capability to measure air showers we are building the **LOFAR Prototype Station** (LOPES) at the site of KASCADE and operate in conjunction with it. The data from a well tested air shower experiment like KASCADE not only allows us to calibrate the radio data with other air shower parameters, it also provides LOPES with starting points for the air shower reconstruction, which simplifies the development process. This will enable us to clarify the nature and properties of radio emission from air showers and provides an energy calibration for future radio air shower experiments. Also LOPES will provide KASCADE with valuable additional information about the air shower, as the radio data and the particle data come from different stages in the evolution of an air shower.

4.3. The Hardware of LOPES

In its first stage LOPES will consist of 10 antennas and will be extended to 100 antennas after successful completion of the first stage. With this LOPES will be sensitive to cosmic rays from 10^{15} to 10^{17} eV

[§]1 $Jy = 10^{-26} W/m^2/Hz$

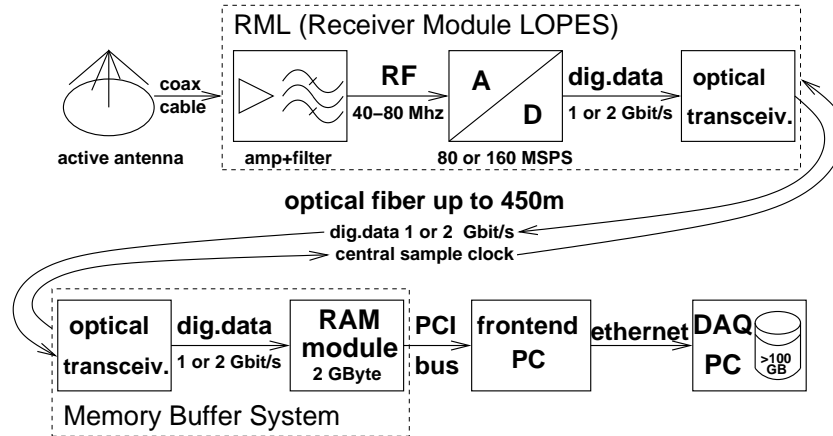


Figure 12. Outline of the hardware, that will be used for LOPES. In the first phase the 80 MSPS / 1 GBit/s configuration will be implemented. In the second phase the 160 MSPS / 2 GBit/s configuration will be implemented, allowing full Nyquist sampling of the 80 MHz.

It will operate in the frequency range of 40–80 MHz, because in this range there are only few strong radio transmitters (the FM radio band is avoided) and the radio emission from air showers are strong compared to the sky noise. As basic element the short dipole antennas, that are currently being developed for LOFAR will be used.

The RF-signal is sampled without the use of a local oscillator (LO) directly at the antenna (see Fig. 12). This prevents the need for long analog signal cables and keeps overall costs low. The signal is sampled with 12-bit ADCs. This gives the necessary dynamic range to detect weak pulses while not saturating the ADC with the Radio Frequency Interference (RFI). In the first stage the ADCs will work at 80 MSPS, allowing 2nd Nyquist sampling of the RF. In the second stage the ADCs will work at 160 MSPS allowing full Nyquist sampling. The sample clock for the ADCs is generated once at a central position and then distributed to all A/D-boards. This allows us to combine the data from all antennas as a phased array and thus enhance the sensitivity.

The digital data is transferred via fiber optic cables to a memory module on a FrontEnd-PC (10 antennas per module). This can store more than half a second of data in a digital ring buffer. After a trigger from KASCADE, the data is read out and sent to a central DAQ-PC, where it can be analyzed online or stored on hard disk.

The hardware for LOPES (active antennas, A/D-boards, memory modules, etc.) is currently being developed at ASTRON in Dwingeloo, Netherlands. First prototypes of the A/D-boards and memory modules are built and being tested.

4.4. Digital RFI Suppression

In February and March 2002 we did first RFI measurements in Dwingeloo and at KASCADE in Karlsruhe. At both sites significant RFI was present, both as narrow band transmissions and short-time pulses. The RFI in Karlsruhe is somewhat stronger but qualitatively the same as in Dwingeloo. An important result is, that no radio pulses coming from the particle detectors or trigger electronics of KASCADE have been detected, as they would be hard to distinguish from air shower emission.

In Fig. 13 one can see the effects of digital RFI suppression. The time series data is Fourier transformed, narrow band RFI is filtered, transformed back to the time domain and data from different simulated antennas is combined. Pulses that get weaker by a large amount can then be identified as RFI and filtered out.

5. CONCLUSION

The KASCADE experiment is taking data since the end of 1995. The EAS observables obtained by KASCADE are sensitive to hadronic interaction models used in simulations to interpret EAS data. At present, the

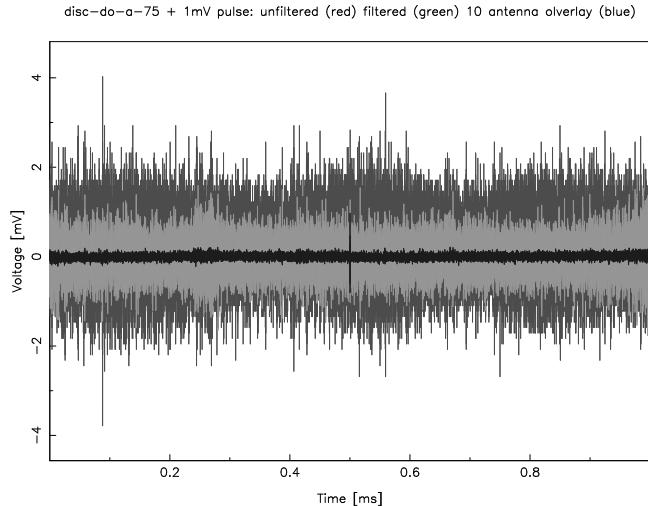


Figure 13. Example of digital RFI Suppression. Time series with added pulse at 0.5 ms (dark grey), after suppression of narrow band RFI (light grey) and after combining 10 antennas as a phased array (black).

combination CORSIKA/QGSJET best describes the measurements. The systematic dependence of the mean logarithmic mass on different observables and models has been investigated. The systematic error for the model QGSJET is in the order of $\Delta \langle \ln A \rangle \approx 0.8$. The reconstruction of individual energy spectra for groups of elements indicate a rigidity dependent cut-off, which explains the *knee* in the all particle cosmic-ray flux spectrum.

The main characteristics of KASCADE-Grande as a joint application of the KASCADE and EAS-TOP detectors are discussed. The apparatus will be completed in 2002, data taking is planned from 2003 to 2005/2006. In three years of effective data taking it will accumulate sufficient statistics up to 10^{18} eV ($\approx 10^3$ events above $5 \cdot 10^{17}$ eV). This experiment will cover an energy range that is poorly known, essentially from old AKENO³⁴ and the lower tail of FLY'S EYE³⁵ data. The task of the experiment is to give a conclusive answer on the structure of the knee, testing the rigidity dependent model up to the energies of the "iron" group. Moreover it will allow to test different hadronic models in an energy range not accessible to accelerators but important for CRs physics. Finally it will provide a bridge to the measurement and interpretation of CRs for experiments working at much higher energies like the Pierre Auger, HIRES or OWL-Airwatch Projects.

We will finish the first stage of LOPES until the end of 2002/beginning of 2003. Early in 2004 we plan to have LOPES running with all 100 antennas. In the case of being successful in measuring radio emission from cosmic ray air showers with sufficient quality in the LOPES test period, we would have the possibility to include this technique as a permanent new component in the KASCADE-Grande experiment. The same technology could then also greatly enhance the sensitivity of other air shower arrays and be applied to LOFAR and other forthcoming digital radio telescopes like the SKA, providing additional detection area for high energy cosmic rays.

ACKNOWLEDGMENTS

The KASCADE experiment is supported by the German Federal Ministry of Education and Research and embedded in collaborative WTZ projects between Germany and Romania (RUM 97/014) and Poland (POL 99/005). The Polish group acknowledges the support by KBN grant no. 5 P03B 133 20. Special thanks are due to INFN for allowing the use of the EAS-TOP equipment to build the Grande array. LOPES is financed by a grant of the German Federal Ministry of Education and Research.

REFERENCES

1. P. Doll et al., Kernforschungszentrum Karlsruhe, Report KfK 4686 (1990).
2. M. Aglietta et al., Nucl. Instr. Meth. A 277 (1989) 23.

3. H. Schieler, "Konzeption, Entwicklung und Test des lokalen Datenerfassungssystems für das strukturierte Detektor-Array von KASCADE", PhD Thesis, University of Karlsruhe, 1996
4. J. Engler et al., Nucl. Instr. and Meth. A 427 (1999) 528.
5. H. Bozdog et al., Nucl. Instr. and Meth. A 465 (2001) 455.
6. P. Doll. et al., Nucl. Instr. and Meth. A 367 (1995) 120.
7. R. Glasstetter et al., Proc. 26th Int. Cosmic Ray Conf., Salt Lake City 1 (1999) 222.
8. J.R. Hörandel et al., Proc. 26th Int. Cosmic Ray Conf., Salt Lake City 1 (1999) 337.
9. M. Roth et al., Proc. 26th Int. Cosmic Ray Conf., Salt Lake City 1 (1999).
10. J.H. Weber et al., Proc. 26th Int. Cosmic Ray Conf., Salt Lake City 1 (1999).
11. M. Aglietta et al., Proc. 26th Int. Cosmic Ray Conf., Salt Lake City 1 (1999).
12. J. Zabierowski et al., Nucl. Instr. and Meth. A 354 (1995) 496.
13. A. Horneffer, "Aufbau eines Flash-ADC Systems und Messung der Zeitstruktur ausgedehnter Luftschauer mit dem KASCADE-Experiment", Diploma Thesis, University of Karlsruhe, 2001
14. H.H. Mielke et al., Nucl. Instr. and Meth. A 360 (1995) 367.
15. H. Rebel et al., J. Phys. G: Nucl. Part. Phys. 21 (1995) 541.
16. T. Antoni et al., Proc. 27th Int. Cosmic Ray Conf., Hamburg 1 (2001).
17. D. Heck et al., Report FZKA 6019 (1998).
18. H. Schieler et al., "The data acquisition system of the KASCADE air shower experiment", Contr. paper to CHEP97, Berlin, (1997).
19. H.J. Mayer, Nucl. Instr. and Meth. A 317 (1992) 339.
20. H.J. Mayer, Nucl. Instr. and Meth. A 330 (1993) 254.
21. A. Haungs et al., Nucl. Phys. B (Proc. Suppl.) 52B (1997).
22. J. Milke et al., Proc. 27th Int. Cosmic Ray Conf., Hamburg 1 (2001) 241.
23. T. Antoni et al., J. Phys. G 25 (1999) 2161.
24. R. Glasstetter et al., Proc. 16th Europ. Cosmic Ray Symp., Alcala de Henares (1998) 563.
25. R. Glasstetter et al., Proc. 26th Int. Cosmic Ray Conf., Salt Lake City 1 (1999) 222.
26. J.R. Hörandel et al., Proc. 26th Int. Cosmic Ray Conf., Salt Lake City 1 (1999) 337.
27. H. Ulrich et al., Proc. 27th Int. Cosmic Ray Conf., Hamburg 1 (2001) 97.
28. J.V. Jelly et al., Nature 205 (1965) 327.
29. H.R. Allan, Prog. in Elem. part. and Cos. Ray Phys. 10 (1971) 171.
30. H. Falcke and P. Gorham, Astropart. Phys., in press, 2002.
31. J.H. Prah, "Radio Emission from Extensive Air Showers", MSc Thesis, University of London, 1971.
32. T. Huege and H. Falcke, Proceedings of the 6th European VLBI Network Symposium, E. Ros, R.W. Porcas, A.P. Lobanov and J.A. Zensus, eds., MPIfR, Bonn, Germany, 2002.
33. J.D. Bregman, Perspectives on Radio Astronomy: Technologies for Large Antenna Arrays, eds. A.B. Smolders & M.P. van Haarlem, 1999.
34. M. Nagano et al., J. Phys. G 10 (1984) 1295.
35. D.J. Bird et al., Astrophys. J., 424 (1994) 491.